applied sciences

MDPI

Review

Positron Emission Tomography in Cerebral Amyloid Angiopathy: A Scoping Review

Marialuisa Zedde [1,2,3,*], Fabrizio Piazza [2,3,4] and Rosario Pascarella [2,3,5]

[1] Neurology Unit, Stroke Unit, Azienda Unità Sanitaria Locale-IRCCS di Reggio Emilia, Viale Risorgimento 80, 42123 Reggio Emilia, Italy
[2] CAA and AD Translational Research and Biomarkers Laboratory, School of Medicine, University of Milano-Bicocca, 20900 Monza, Italy; fabrizio.piazza@unimib.it (F.P.); rosario.pascarella@aulss5.veneto.it (R.P.)
[3] SINdem Study Group "The Inflammatory Cerebral Amyloid Angiopathy and Alzheimer's Disease Biomarkers"
[4] iCAβ International Network
[5] Neuroradiology Unit, Ospedale Santa Maria della Misericordia, AULSS 5 Polesana, 45100 Rovigo, Italy
* Correspondence: zedde.marialuisa@ausl.re.it or marialuisa.zedde@gmail.com

Abstract: Background/Objectives: Cerebral amyloid angiopathy (CAA) is one of the most prevalent small vessel diseases (SVDs). Its diagnostic criteria rely mainly on neuroimaging markers, in particular using Magnetic Resonance Imaging (MRI), as pathology-based diagnoses are only occasionally available. Amyloid PET is frequently used to assess parenchymal amyloid deposition in Alzheimer's disease (AD), but amyloid tracers are not specific to vascular and parenchymal amyloids. The aim of this scoping review is to assess the usefulness of amyloid PET imaging in CAA. Methods: A systematic literature search was performed, aiming to assess amyloid PET performance in the following situations: (I) CAA-related intracerebral hemorrhage (ICH) and convexal subarachnoid hemorrhage; (II) pathology-proven CAA; (III) CAA-related inflammation; (IV) hereditary CAA. Results: A total of 52 studies were retrieved, including three systematic reviews, and from these, a specific selection was taken according to each objective, confirming the diagnostic value of amyloid PET added to MRI and clinical information in all the selected situations, although with some limitations. Conclusions: Amyloid PET reliably detects increased global and region-specific amyloid deposition in CAA patients, with a characteristic occipital-predominant pattern. Continued advancements in tracer development and imaging methodologies are needed to increase specificity.

Keywords: cerebral amyloid angiopathy; CAA; amyloid PET; MRI; cortical superficial siderosis; microbleeds; WMHs; CAA-related inflammation; hereditary CAA

check for updates

Academic Editor: Sarmistha Mitra

Received: 11 February 2025
Revised: 30 March 2025
Accepted: 2 April 2025
Published: 3 April 2025

Citation: Zedde, M.; Piazza, F.; Pascarella, R. Positron Emission Tomography in Cerebral Amyloid Angiopathy: A Scoping Review. *Appl. Sci.* **2025**, *15*, 3973. https://doi.org/10.3390/app15073973

Copyright: © 2025 by the authors. Licensee MDPI, Basel, Switzerland. This article is an open access article distributed under the terms and conditions of the Creative Commons Attribution (CC BY) license (https://creativecommons.org/licenses/by/4.0/).

1. Introduction

Cerebral amyloid angiopathy (CAA) is one of the small vessel diseases (SVDs) [1–3] with the highest prevalence in the population, and is responsible for multiple consequences, including brain bleeding (convexal subarachnoid hemorrhage and intraparenchymal hemorrhage), cognitive impairment and dementia, and gait disturbances [4]. Its prevalence increases with the age of the population, but the current diagnostic criteria include an age threshold of 50 years, which makes the characteristics of the disease even more significant [5]. CAA is a subtype of SVD that affects the arterioles, capillaries, and leptomeningeal and cortical venules, in which the progressive deposition of non-water-soluble fragments of beta amyloid, in particular, the fragment 1–42, determines the progressive subversion of the structure of the vessel wall, which impacts the vessels' function and structural integrity [4].

CAA is most frequently associated with the other most prevalent amyloid-related brain disease, namely, Alzheimer's disease (AD) [4]. The co-presence of CAA and AD in the same subject occurs in up to 80% of cases in histopathological series, although this association is reduced if only moderate–severe CAA is considered [4,6]. The association with AD represents an important element both for the possible overlapping of clinical manifestations and natural history, as well as for diagnostic aspects. In fact, if it is known that a significant proportion of patients with AD have signs of SVD on Magnetic Resonance Imaging (MRI), expressed by both hemorrhagic and non-hemorrhagic markers [7], it is equally true that the diagnosis of AD is made, in accordance with the ATN criteria, on the basis of the demonstration of alteration of beta amyloid (reduced levels in the cerebrospinal fluid—CSF—or cerebral hyperaccumulation in positron emission tomography—PET—with amyloid tracers) and of the tau protein (increased levels in the CSF or tau PET with pathological results) [8]. The coexistence of CAA and AD makes it highly probable that the dosage of neurodegeneration biomarkers in the cerebrospinal fluid and PET with amyloid tracers are altered in patients with CAA, although it is impossible to reliably determine to which of the two diseases the findings can be attributed, vascular or neurodegenerative. In this context, it is also possible to postulate the existence of subgroups of patients with pure CAA and pure AD. Since CAA, in the absence of a previous history of intracerebral hemorrhage (ICH) and clinical manifestations that fall within the current diagnostic criteria (e.g., cognitive impairment and transient focal neurological episodes), can be diagnosed with a sensitivity and specificity of approximately 60%, the availability of diagnostic support with techniques other than MRI could be useful [5]. The number of studies that have explored the role of PET with amyloid tracers in CAA is few, and the number of patients is also limited; furthermore, in these studies, there is no contemporary assessment of CSF biomarkers that can help to define the co-presence of more than one neurodegenerative disease [9]. Despite these limitations, the approach appears promising, particularly in patients with lobar ICH, in which the histopathology is consistent with a diagnosis of underlying CAA in only 50% of cases [6]; and in patients with inflammatory manifestations, such as CAA-related inflammation, which are very similar to the amyloid-related imaging abnormalities described, to a lesser extent, as spontaneous events, and to a greater extent, as iatrogenic events in AD patients treated with immunotherapy [10–15].

The aim of this scoping review is to assess the role and the potential application of PET with amyloid tracers in CAA patients, highlighting the strengths and limitations of the available studies and identifying future perspectives.

2. Materials and Methods

This scoping review was performed according to previously described principles [16] and to the Preferred Reporting Systems for Systematic Reviews and Meta-Analyses Extension for Scoping Reviews (PRISMA-ScR) framework [17]. The protocol of this review was not registered in PROSPERO, due to the lack of acceptance of scoping reviews.

2.1. Definitions

2.1.1. Cerebral Amyloid Angiopathy (CAA)

Since most studies enrolled patients before the publication of the Boston 2.0 criteria [5], the definition of possible, probable, and definite CAA was made based on the Boston 1.5 criteria [18], as shown in Table 1. Both sporadic and hereditary CAA have been included.

Table 1. CAA diagnostic criteria v. 1.5 [18].

Diagnostic Category	Criteria
Definite CAA	Full post-mortem examination demonstrating the following: • Lobar, cortical, or cortical–subcortical hemorrhage • Severe CAA with vasculopathy • Absence of other diagnostic lesion
Probable CAA with supporting pathology	Clinical data and pathologic tissue (evacuated hematoma or cortical biopsy) demonstrating the following: • Lobar, cortical, or cortical–subcortical hemorrhage (including ICH and/or CMB) • Some degree of CAA in specimen • Absence of other diagnostic lesion
Probable CAA	Clinical data and MRI or CT demonstrating the following: • Multiple hemorrhages (ICH, CMB) restricted to lobar, cortical, or cortical–subcortical regions (cerebellar hemorrhage allowed) OR • Single lobar, cortical, or cortical–subcortical hemorrhage and cSS (focal or disseminated) • Age $\geq$ 55 years • Absence of other cause of hemorrhage or cSS
Possible CAA	Clinical data and MRI or CT demonstrating the following: • Single lobar, cortical, or cortical–subcortical ICH, CMB OR • Presence of cSS (focal or disseminated) • Age $\geq$ 55 years • Absence of other cause of hemorrhage or cSS

CMB: cerebral microbleed; cSS: cortical superficial siderosis.

2.1.2. Positron Emission Tomography with Amyloid Tracers

PET imaging with [^{11}C]Pittsburgh compound B (PiB) [19], [^{18}F]florbetapir [20], or [^{18}F]flutemetamol [21] tracers has been shown to measure the burden and location of fibrillar cerebrovascular (in addition to parenchymal) b-amyloid deposits [20,21]. While it is clear that CAA is detectable by amyloid-PET [19–21], the available tracers have no selectivity for vascular or parenchymal amyloids.

2.2. Objectives

The main objectives of this scoping review are an analysis of the literature on amyloid PET performance in the following situations: (I) CAA-related ICH and convexal subarachnoid hemorrhage; (II) pathology-proven CAA; (III) CAA-related inflammation; (IV) hereditary and iatrogenic CAA.

2.3. Literature Search

A systematic review was conducted of published papers reporting abdominal aortic involvement in patients with FMD, following the Meta-Analyses and Systematic Reviews of Observational Studies (MOOSE) group guidelines [22]. We searched the PubMed and EMBASE databases for studies addressing abdominal aortic status in FMD, from inception to 17 September 2024. We used the following keywords for PubMed: "(angiopathy, cerebral amyloid [MeSH Terms]) AND (positron emission tomography [MeSH Terms])". We excluded patients with thoracic aortic dissection and traumatic dissection. In addition, we applied forward and backward citation tracking to improve the results. All studies presenting original data relating to the topic of the review were included. We limited the

selection to English studies, and excluded studies on nonhuman subjects and case reports or cases. Abstracts presented at relevant scientific meetings were excluded because of a lack of relevant information. We avoided including duplicated datasets. Two investigators (MZ, RP) independently screened the papers retrieved in the literature search, performing this according to previously detailed criteria, and a third investigator (F.P.) was involved to resolve disagreements. The NIH Quality Assessment Tool for Observational Cohort and Cross-Sectional Studies [23] was used to evaluate each eligible publication. The following information was extracted: authors, year of publication, number of patients with possible/probable/definite CAA, and MRI and PET findings. In the case of missing values, we tried to derive them whenever it was possible [23]. Disagreements between the two reviewers were addressed and resolved by consensus.

3. Results

The literature search retrieved 109 papers; following screening and reference checks, a total of 52 papers suitable for data extraction were identified. This selection process is summarized in Figure 1.

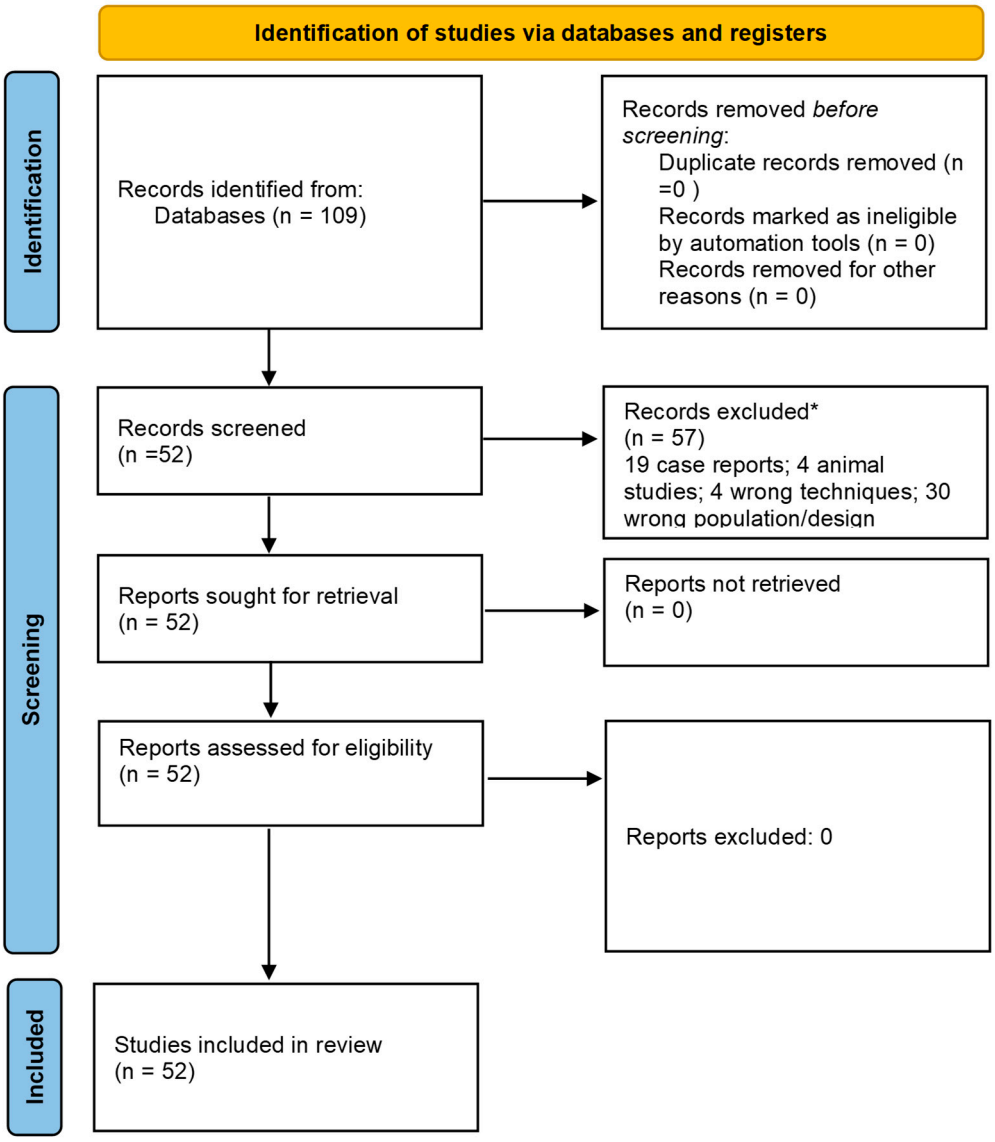


Figure 1. Prisma flow diagram [24]. *: reasons for the excluded papers are reported below.

All the selected papers were analyzed in order to answer the previously identified objectives, and a further selection of papers was performed for each of the four objectives.

3.1. Overview

Amyloid PET imaging has consistently shown an increased global amyloid burden in patients with CAA, and three systematic reviews and a meta-analysis have addressed some general questions. Farid et al. [25] evaluated global amyloid-beta deposition using [^{11}C]PiB PET. They reported significantly elevated global amyloid uptake in symptomatic CAA patients compared to healthy controls and patients with deep intracerebral hemorrhage (ICH). The findings confirmed widespread amyloid deposition in CAA [25]. Similarly, a meta-analysis [26] corroborated these findings, showing that the global amyloid burden is substantially higher in CAA patients than in controls. The effect size for increased global uptake was significant (1.18, 95% CI: 1.08–1.28, $p < 0.0001$), indicating the utility of amyloid PET in diagnosing CAA and differentiating it from other cerebrovascular conditions.

Another relevant issue is regional amyloid deposition, with occipital predominance being more common in CAA than in AD. Occipital predominance of amyloid deposition is a hallmark feature of CAA, and distinguishes it from AD. A study by Charidimou et al. [26] analyzed the occipital-to-global amyloid uptake ratio, and found that CAA patients exhibited significantly higher ratios than AD patients. This regional preference aligns with the clinical manifestations of CAA, such as occipital lobe hemorrhages and visual disturbances.

A related study [9] explored the relationship between regional amyloid burden and symptomatic presentations in CAA, confirming that amyloid deposition is disproportionately higher in posterior regions, particularly the occipital lobes, compared to anterior cortical regions. This occipital predilection helps to differentiate CAA from AD, where amyloid distribution is more diffuse. The occipital-to-global uptake ratio was also validated in the previously cited meta-analysis [26], where CAA patients demonstrated a higher ratio (1.10, 95% CI: 1.03–1.19, $p = 0.009$) compared to AD patients, further emphasizing the diagnostic value of regional amyloid imaging markers.

The main findings of the three published systematic reviews are summarized in Table 2.

Table 2. Findings of three published systematic reviews on amyloid PET and CAA.

Reference	Population	Details	Findings	Comments
Farid et al., 2017 [25]	Probable CAA: 129 Possible CAA: 65 Healthy controls (HCs): 30	Probable CAA was diagnosed using Boston criteria [18] and amyloid PET imaging with [^{11}C]PiB tracer. Possible CAA was diagnosed with suspected but unconfirmed CAA, due to lack of definitive imaging or pathology. HCs were matched by age and sex to CAA patients for comparison.	- Significantly higher global [^{11}C]PiB PET uptake in CAA patients compared to controls and deep ICH patients. - Regional amyloid predominance in occipital lobes.	The focus was global and regional amyloid deposition in CAA. The findings support the diagnostic utility of amyloid PET in identifying CAA-specific amyloid patterns. Occipital predominance aids in differentiating CAA from other amyloid-related diseases, such as AD.
Charidimou et al., 2018 [26]	CAA (total): 155 AD: 320 HC: 80	CAA includes both probable and possible CAA cases; amyloid PET imaging was conducted with different tracers. AD patients were included for comparison of amyloid patterns between CAA and AD populations. Controls were used to establish baseline amyloid uptake and regional distribution.	- Global amyloid burden higher in CAA vs. controls (effect size: 1.18, 95% CI: 1.08–1.28, $p < 0.0001$). - Occipital-to-global uptake ratio significantly higher in CAA vs. AD (mean ratio: 1.10, 95% CI: 1.03–1.19, $p = 0.009$).	A systematic review and meta-analysis of amyloid PET in CAA and AD. The findings confirm global and regional amyloid deposition patterns as key diagnostic markers. The findings highlight the occipital-to-global ratio as a differentiating feature between CAA and AD, improving diagnostic specificity.

Table 2. *Cont.*

Reference	Population	Details	Findings	Comments
Charidimou et al., 2017 [9]	Probable CAA: 52 AD: 75 HC: 20	Probable CAA was defined by Boston criteria [18], and confirmed by imaging findings (including MRI and [^{11}C]PiB PET). AD patients were included to investigate differences in amyloid regionality, particularly occipital involvement. HCs were used to analyze regional amyloid patterns compared to CAA patients.	- Occipital lobe amyloid deposition disproportionately higher compared to other cortical regions. - Regional amyloid patterns correlated with clinical manifestations (e.g., lobar hemorrhages, visual disturbances).	- The findings establish the occipital amyloid burden as a hallmark of CAA. - The findings suggest that regional amyloid patterns can predict clinical symptoms, and may guide targeted interventions or prognosis in patients with CAA.

In total, the three systematic reviews provided data on 367 CAA patients (probably with overlapping studies among the three papers), 360 AD patients, and 242 HCs. The overlapping and potential duplication of data among studies may affect the strength of the conclusions.

3.2. CAA-Related ICH and SAH

Studies consistently demonstrate that patients with probable CAA exhibit elevated amyloid uptake on PET imaging, particularly in the occipital regions. For example, Romoli et al. [27] highlighted a 40% higher occipital standardized uptake value ratio (SUVR) in probable CAA compared to AD, underscoring the regional specificity of amyloid deposition in CAA. Conversely, Michiels et al. [28] reported an occipital-to-global SUVR of 1.8 ± 0.3, significantly higher than in AD patients ($p < 0.001$).

Probable CAA patients with ICH consistently show higher regional amyloid burdens. Amyloid PET findings predicted ICH recurrence with 85% sensitivity and 82% specificity, indicating its prognostic utility [29]. Similarly, a significant association was found between recurrent ICH and elevated global SUVR (1.7 ± 0.3, $p = 0.02$) [30].

Amyloid PET has proven effective in distinguishing probable CAA from mimicking conditions like hypertensive ICH, with an area under the curve (AUC) of 0.87 for amyloid PET in differentiating CAA from hypertensive ICH [31]. These findings support amyloid PET as a valuable diagnostic adjunct when traditional imaging is inconclusive.

The Boston criteria for CAA diagnosis [5,18] are further refined by amyloid PET, particularly for probable cases with lobar ICH. In fact, one study found that 73% of probable CAA cases demonstrated occipital-dominant amyloid deposition, significantly higher than in AD patients ($p < 0.001$) [32]. This regional specificity helps to differentiate CAA from other amyloidopathies and guides patient management.

Amyloid PET findings correlate with the distribution and burden of cerebral microbleeds in probable CAA, with a strong correlation ($r = 0.62$, $p < 0.001$) between occipital amyloid deposition and lobar microbleeds [33], and a higher amyloid SUVR in recurrent ICH cases [34].

Amyloid PET enhances the sensitivity of CAA diagnosis and helps to stratify patients based on ICH risk. For example, Planton et al. [35] reported an 87% sensitivity and 78% specificity for diagnosing probable CAA in ICH patients.

The main findings of the selected studies are summarized in Table 3.

Table 3. Findings of selected studies on probable and possible CAA and amyloid PET.

Reference	Probable CAA/ICH	Possible CAA	Controls	Key Findings
Gokcal et al., 2022 [36]	58	20	32	Probable CAA patients showed a 1.5-fold increase in occipital amyloid PET SUVR compared to controls ($p < 0.01$).
Romoli et al., 2024 [27]	42	15	30	Probable CAA patients had a 40% higher occipital SUVR compared to Alzheimer's patients ($p < 0.001$), which correlated with recurrent lobar ICH.
Kim et al., 2018 [32]	64	25	35	Out of all probable CAA cases, 73% showed occipital-predominant amyloid uptake, compared to 18% of Alzheimer's cases ($p < 0.001$).
Baron et al., 2014 [33]	40	18	28	A strong correlation was found between occipital amyloid uptake and lobar microbleeds (r = 0.62, $p < 0.001$).
Tsai et al., 2021 [29]	52	22	29	An increased regional amyloid burden in probable CAA predicted ICH recurrence with 85% sensitivity and 82% specificity.
Raposo et al., 2017 [37]	48	16	31	Probable CAA patients showed a 2-fold higher occipital-to-global SUVR compared to possible CAA patients ($p < 0.01$).
Ly et al., 2015 [38]	39	12	25	Amyloid PET uptake was significantly higher in probable CAA with lobar microbleeds compared to hypertensive ICH ($p < 0.001$).
Yost et al., 2019 [31]	46	15	24	Amyloid PET differentiated probable CAA from hypertensive ICH with an AUC of 0.87 (95% CI: 0.81–0.92, $p < 0.001$).
Michiels et al., 2022 [28]	57	23	30	The occipital-to-global amyloid ratio was higher in probable CAA than Alzheimer's disease (mean SUVR 1.8 ± 0.3 vs. 1.2 ± 0.4, $p < 0.001$).
Gurol et al., 2016 [39]	44	18	26	Probable CAA patients showed a significant amyloid burden (SUVR 1.6 ± 0.2) compared to controls ($p < 0.001$), which was correlated with ICH.
Tsai et al., 2019 [30]	51	20	29	A higher amyloid burden was found in recurrent ICH cases (SUVR 1.7 ± 0.3, $p = 0.02$); the occipital SUVR was elevated in probable CAA.
Planton et al., 2020 [35]	48	14	28	Amyloid PET had 87% sensitivity and 78% specificity for diagnosing probable CAA in ICH patients compared to controls.
Jang et al., 2019 [40]	38	10	20	The occipital SUVR was 50% higher in probable CAA patients compared to hypertensive ICH patients ($p < 0.001$).
Raposo et al., 2019 [34]	47	18	27	Regional amyloid deposition was found to be correlated with ICH burden and distribution (r = 0.58, $p < 0.01$).

3.3. Pathology-Proven CAA

The studies consistently identify occipital-dominant amyloid deposition as a hallmark of probable CAA. For example, Pyun et al. [41] reported an SUVR of 1.65 ± 0.2 in the occipital lobe of probable CAA patients, significantly higher than in AD patients or controls ($p < 0.001$). Similarly, McCarter et al. [42] found an even higher occipital SUVR (1.7 ± 0.3) in probable CAA cases, emphasizing the diagnostic value of this regional amyloid pattern.

Recurrent ICH episodes in probable CAA are linked to higher regional amyloid deposition. Pyun et al. [41] demonstrated that PET imaging predicted ICH recurrence with 83% sensitivity, highlighting its prognostic utility. Furthermore, another study [43] reported a significant correlation (r = 0.58, $p < 0.01$) between regional amyloid uptake and cortical microbleeds, a critical marker of disease severity.

The study of Kim et al. [32] focused on the role of cSS in CAA pathology, noting that probable CAA patients with cSS had a higher occipital amyloid SUVR and greater posterior

cortical atrophy than those without cSS. This suggests that CSS exacerbates both amyloid pathology and structural brain damage.

Across studies, amyloid PET demonstrated robust differentiation between CAA and AD, with an AUC of 0.89 ($p < 0.001$) for PET imaging in distinguishing probable CAA from AD [42]. The occipital-to-global SUVR was particularly useful, with CAA showing occipital-predominant uptake, compared to the more diffuse pattern seen in AD.

PET imaging consistently matched with vascular amyloid deposition in CAA patients, concentrated in the occipital and posterior cortical regions. This pattern correlates with clinical features, including recurrent lobar ICH and cortical microbleeds. A single study [43] also linked increased amyloid burden with disease progression, suggesting that PET findings may serve as biomarkers for tracking disease severity.

The main findings are summarized in Table 4.

Table 4. Findings of selected studies on pathology-proven CAA and amyloid PET.

Study	Probable CAA with ICH (N)	Possible CAA (N)	Controls (Healthy/AD)	Pathological Data	Key Findings
Pyun et al., 2024 [41]	56	18	34	Higher amyloid deposition in occipital regions; SUVR 1.65 ± 0.2 ($p < 0.001$).	PET imaging predicted ICH recurrence with 83% sensitivity. Occipital-to-global SUVR distinguished CAA from AD.
Buciuc et al., 2021 [43]	62	20	30	Regional amyloid correlated with cortical microbleeds (r = 0.58, $p < 0.01$).	Amyloid burden highest in occipital lobes in CAA patients, correlating with disease severity and microbleeds.
McCarter et al., 2021 [42]	59	21	28	Occipital-dominant SUVR in probable CAA (1.7 ± 0.3) vs. AD. Atrophy patterns also noted in posterior regions.	PET accurately differentiated probable CAA from AD with AUC of 0.89 ($p < 0.001$).
Kim et al., 2018 [32]	48	16	30	cSS associated with increased occipital amyloid burden.	Probable CAA with cSS showed higher occipital amyloid and greater atrophy in posterior cortices compared to non-cSS.

3.4. Hereditary CAA

Five papers collectively provided a deeper understanding of hereditary CAA subtypes, emphasizing their unique clinical and imaging profiles. Hereditary CAA results from mutations such as Dutch-type CAA (APP E693Q), APP duplications, ATTR mutations, and others. PET imaging with Pittsburgh Compound B—[^{11}C]Pib—serves as a consistent marker for amyloid pathology across all forms of hereditary CAA. In particular, two studies focused on hereditary ATTR amyloidosis, providing insights into amyloid-related imaging features such as cSS and CMBs. An elevated amyloid burden detected via [^{11}C]PiB PET highlights parallels with hereditary CAA in amyloid deposition [44,45].

Studies on Dutch-Type CAA [46,47] identified frequent cortical microinfarcts, extensive WMH, and CMBs, underscoring the impact of this mutation on cerebrovascular integrity. In addition, a strong correlation was proposed between amyloid deposition, as measured by PiB PET, and imaging markers of cerebrovascular injury.

Patients with hereditary APP duplication exhibited severe WMH, cSS, and numerous CMBs. Notably, [^{11}C]Pib PET demonstrated extensive amyloid deposition, including parenchymal areas beyond blood vessels. This finding highlights the diffuse impact of APP mutations [48].

The main findings are summarized in Table 5.

Table 5. Findings of selected studies on hereditary CAA and amyloid PET.

Reference	Population	Hereditary CAA	Imaging Findings	PET Findings
Sekijima et al., 2016 [44]	20 patients with hereditary ATTR amyloidosis and 20 healthy controls	ATTR amyloidosis	Increased cortical cSS in patients (45% vs. 0% in controls); higher number of cerebral microbleeds in patients (median 18 vs. 0 in controls)	Higher Pittsburgh Compound B—[^{11}C]Pib—retention in patients, indicating increased amyloid deposition
Chatterjee et al., 2021 [46]	50 patients with hereditary Dutch-type CAA and matched controls	Dutch-type mutation	Extensive cortical microinfarcts (detected via advanced imaging) and higher white matter hyperintensities (WMHs); consistent presence of CMBs	Elevated amyloid load shown by [^{11}C]PiB PET
Schultz et al., 2019 [47]	12 patients with hereditary Dutch-type CAA and 12 controls	Dutch-type mutation	Increased prevalence of cSS (50% vs. 0%) and higher WMH volume	Increased PiB retention in patients, correlating with cSS and WMH volume
Huang et al., 2019 [48]	15 patients with hereditary CAA due to APP duplication and matched controls	APP duplication	Severe WMHs, numerous cortical CMBs, and cSS	Increased PiB uptake in affected patients, with amyloid deposition extending beyond vessels
Takahashi et al., 2023 [45]	15 patients with hereditary Dutch-type CAA and 15 controls	ATTR amyloidosis	Increased WMHs and presence of cSS in 40% of patients	Higher PiB retention in patients, consistent with amyloid pathology

3.5. CAA-Related Inflammation

CAA-ri is an uncommon and often reversible encephalopathy, characterized by an inflammatory response to amyloid-beta deposits within the cerebral vasculature. Few studies have addressed the performance of amyloid PET in patients with this condition [49–51]. The first one [49] examined 12 patients with CAA-ri, highlighting MRI findings on FLAIR and gradient-recalled echo (GRE) sequences indicative of vascular inflammation and damage associated with CAA-ri, but without quantitative details on amyloid PET imaging. Another group [50] studied eight patients with asymmetric white matter hyperintensities, cortical swelling, and leptomeningeal enhancement, along with microbleeds identified on susceptibility-weighted imaging (SWI) on MRI. Notably, amyloid PET imaging demonstrated elevated uptake in cortical regions, suggesting significant amyloid deposition contributing to the inflammatory process. A third study [51] assessed 10 patients with CAA-ri. MRI findings included extensive white matter hyperintensities, cortical edema, and leptomeningeal enhancement, with microbleeds observed on GRE sequences. Amyloid PET showed increased cortical uptake, corroborating amyloid involvement, while FDG-PET revealed hypometabolism in affected regions, indicating functional impairment associated with inflammatory changes.

The main findings are summarized in Table 6.

Table 6. Findings of selected studies on CAA-ri and amyloid PET.

Reference	Population	Imaging Findings	PET Findings
Carmona-Iragui et al., 2016 [49]	12 patients with CAA-ri	MRI: leukoencephalopathy; multiple cortical and subcortical hyperintensities on FLAIR; microbleeds on GRE sequences	Not specified
Renard et al., 2018 [50]	8 patients with CAA-ri	MRI: asymmetric white matter hyperintensities, cortical swelling, leptomeningeal enhancement; microbleeds on SWI	Amyloid PET: elevated uptake in cortical regions
Renard et al., 2018 [51]	10 patients with CAA-ri	MRI: extensive white matter hyperintensities, cortical edema, leptomeningeal enhancement; microbleeds on GRE	Amyloid PET: increased cortical uptake; FDG-PET: hypometabolism in affected regions

FLAIR: Fluid-Attenuated Inversion Recovery; GRE: gradient-recalled echo.

4. Discussion

CAA is a cerebrovascular condition characterized by amyloid-β deposition in the walls of cerebral small vessels, leading to an increased risk of ICH. The Boston criteria are commonly used to diagnose CAA, categorizing cases into "probable" or "possible" based on clinical and imaging findings [5,15]. Probable CAA is often associated with lobar ICH, a hallmark of the disease [5,15]. Amyloid PET imaging has emerged as a valuable tool for detecting amyloid deposition in vivo, aiding in the diagnosis and understanding of CAA. It is a technique that provides a more direct molecular imaging biomarker to identify cerebrovascular amyloid in vivo, which would have clinical implications for accurate early diagnosis, dementia and stroke risk stratification (in ICH and anticoagulation-related ICH), and future disease-modifying strategies [52]. A comprehensive understanding of findings from systematic reviews and meta-analyses highlights the diagnostic and clinical implications of amyloid PET in patients with CAA.

Amyloid PET imaging can detect amyloid-β deposition in the cerebral vasculature, providing supportive evidence for CAA diagnosis. Studies have shown that patients with probable CAA and ICH exhibit increased amyloid uptake on PET imaging, particularly in the occipital lobes. This regional distribution differs from that observed in AD, where amyloid deposition is more diffuse. The correlation between amyloid PET findings and CAA-related ICH suggests that amyloid imaging can enhance diagnostic accuracy and potentially guide therapeutic decisions.

Systematic reviews have consistently reported that global amyloid-beta deposition is significantly elevated in patients with symptomatic CAA compared to healthy controls and patients with deep intracerebral hemorrhage [24–26]. For instance, Charidimou et al. [26] conducted a meta-analysis examining global amyloid PET uptake in CAA patients. The study found a significant increase in the global amyloid burden, with an effect size of 1.18 (95% CI: 1.08–1.28, $p < 0.0001$). This finding underscores the extensive amyloid deposition present in the vasculature of CAA patients, a feature that distinguishes the disease from other non-amyloid vascular conditions. Furthermore, amyloid PET imaging has been used to compare amyloid deposition between CAA and AD. Although the global amyloid burden is generally lower in CAA than in AD, the distinct regional distribution patterns in CAA provide essential diagnostic insights. Unfortunately, pathological studies have not found evidence that a pathologically confirmed regional CAA burden contributes significantly to proximal antemortem regional PiB-PET signal in patients with cognitive decline and without previous ICH, suggesting that amyloid PET imaging for the measurement of cortical amyloid burden is unconfounded by CAA on a lobar level [42]. Similar information is not available for patients with severe CAA phenotypes.

A hallmark of CAA is preferential amyloid deposition in the occipital lobes. The meta-analysis by Charidimou et al. [26] also examined the occipital-to-global uptake ratio, a key metric for assessing the regional distribution of amyloids. When comparing CAA to AD patients, CAA patients exhibited a significantly higher occipital-to-global uptake ratio (mean ratio of 1.10, 95% CI: 1.03–1.19, $p = 0.009$). This finding aligns with the clinical presentation of CAA, where occipital lobe-related symptoms, such as visual disturbances and lobar hemorrhages, are more common. These regional differences in amyloid distribution are diagnostically valuable. For example, amyloid PET findings combined with MRI markers, such as cSS or CMBs, enhance the specificity of CAA diagnosis.

Several systematic reviews have explored the prevalence of CAA in different populations using both imaging and pathological studies. Findings suggest that imaging-based methods, including amyloid PET, may underestimate the prevalence of CAA compared to pathological methods. A systematic review and meta-analysis reported that in patients with AD, the prevalence of CAA was 48% when determined by pathology, but only 22% when

identified using imaging techniques. Similarly, in the general population, CAA prevalence was reported as 23% by pathology and 7% by imaging [6,53]. These discrepancies highlight the limitations of current amyloid PET tracers, which are not specific to vascular amyloid deposits. The inability to distinguish between vascular and parenchymal amyloid deposits remains a critical challenge in accurately diagnosing CAA.

Amyloid PET imaging has significant clinical applications in the management of CAA. First, it provides prognostic information by identifying patients who are at risk of recurrent hemorrhages or progressive cognitive decline. Higher amyloid burdens have been correlated with more severe disease phenotypes and poorer outcomes. Second, amyloid PET enhances the differentiation of CAA from other amyloid-related disorders, such as Alzheimer's disease, especially when MRI findings are inconclusive. For example, the occipital-predominant amyloid deposition seen in CAA is distinct from the more diffuse patterns typically observed in AD. This distinction can guide clinical decision-making and inform therapeutic strategies. Finally, amyloid PET imaging is being used to evaluate the effectiveness of emerging therapies targeting amyloid-beta. Clinical trials investigating amyloid-reducing agents rely on imaging markers, including PET, to assess treatment efficacy.

In AD patients, there is reliable pathological information on the accuracy of in vivo [^{18}F]florbetapir PET and histopathology [54,55]. Most data come from studies on end-of-life subjects with advanced disease, in which autopsy is anticipated shortly after PET imaging, and with the specific goal of demonstrating efficacy. Unfortunately, these studies have a selection bias, considering only patients at the extreme ends of the β-amyloid spectrum (either no or frequent neuritic plaque densities, according to CERAD criteria [56]), limiting the applicability of the proposed high test sensitivity and specificity. In both AD and AA, patients that are candidates for functional imaging are those in the early stages of disease development with borderline β-amyloid pathology, as well as patients with preserved cognition. The GE067-026 trial demonstrated 91% sensitivity and 90% specificity of [^{18}F]flutemetamol PET by a majority read for the presence of moderate or frequent plaques [57]. The probability of an abnormal [^{18}F]flutemetamol scan increased with neocortical plaque density and AD diagnosis. The majority of PET assessments accurately reflected the amyloid plaque burden, in 90% of cases. Although tracer retention was best associated with amyloids in neuritic plaques, amyloid in diffuse plaques and CAA best explained three [^{18}F]flutemetamol positive cases with mismatched (sparse) neuritic plaque burden. Advanced cortical atrophy was associated with the seven false negative [^{18}F]flutemetamol images. The interpretation of images from pathologically equivocal cases was associated with low reader confidence and inter-reader agreement. Our results provide supporting evidence that amyloids in neuritic plaque burdens are the primary form of β-amyloid pathology detectable with [^{18}F]flutemetamol PET imaging. Interestingly, a retrospective study on probable CAA patients categorized as having cSS or not focused on the atrophy pattern [32]. In this study, ten patients with probable CAA were cSS-negative and negative for amyloids on PET imaging. In addition, the cSS+ group exhibited an AD-like atrophy pattern, involving the precuneus, posterior cingulate, parietotemporal, superior frontal, and medial temporal areas, suggesting that a subgroup of patients with probable CAA reflects a CAA phenotype that shares pathologic hallmarks with AD, providing insight into the CAA-to-AD continuum.

Non-hemorrhagic manifestations of CAA, such as CAA-related inflammation or ARIA-like events, ARIA being an acronym for Amyloid-related Imaging Abnormalities, represent a relevant and emerging issue, making CAA the spontaneous model of a mostly iatrogenic phenomenon in immunotherapy trials for AD [10–15]. The relevance of biomarkers and PET imaging in these patients is high, and ongoing registries will provide data on large and

homogeneous cohorts. Collectively, these studies underscore the importance of advanced imaging modalities in diagnosing CAA-ri. MRI findings, such as white matter hyperintensities, cortical swelling, and leptomeningeal enhancement, along with microbleeds, are characteristic of CAA-ri. Amyloid PET imaging further aids in identifying amyloid deposition, supporting the diagnosis. FDG-PET can provide additional information regarding metabolic activity in affected brain regions. Early recognition of these imaging features is crucial for prompt diagnosis and treatment of CAA-ri, potentially leading to better clinical outcomes. Future research should focus on longitudinal imaging studies to monitor disease progression and response to therapy, as well as exploring the underlying mechanisms driving inflammation in CAA.

Amyloid PET imaging is also a relevant issue in patients with hereditary CAA, but studies addressing this issue are scarce. This could be due to the fact that the diagnosis is mainly obtained, in symptomatic and in pre-symptomatic cases, through genetic testing. The subtypes of hereditary CAA that have been tested are those due to APP mutations [48], those due to ATTR mutations [44,45], and Dutch-Type Hereditary CAA [46,47]. Cortical superficial siderosis, WMH, and cerebral microbleeds are consistent across hereditary CAA subtypes. However, APP duplication cases have demonstrated more extensive parenchymal amyloid deposition. PiB PET is a valuable tool for assessing amyloid pathology, with elevated uptake consistently correlating with disease severity. Studies underscore the heterogeneity of hereditary CAA, with distinct imaging and pathological profiles for Dutch-type and APP duplication subtypes. PET imaging serves as a vital adjunct to MRI in diagnosing and monitoring disease progression. Future research should explore targeted interventions and the prognostic implications of these findings.

Despite its utility, amyloid PET imaging faces several limitations. Current tracers, such as [^{18}F]florbetapir, [^{18}F]florbetaben, and [^{11}C]PiB, have high sensitivity for amyloid-beta, but lack specificity for vascular amyloid deposits. This limitation complicates the distinction between CAA and other conditions with amyloid pathology. Furthermore, variability in imaging protocols and analysis methods across studies contributes to inconsistent findings. Future research should focus on developing advanced PET tracers with higher specificity to vascular amyloids. Emerging tracers targeting amyloid-beta in vascular walls could significantly enhance the diagnostic accuracy of CAA. Additionally, integrating amyloid PET with multi-modal imaging approaches, such as tau PET and advanced MRI techniques, may provide a more comprehensive assessment of amyloid-related pathology.

Standardization of imaging protocols and analysis techniques is another critical area for improvement. Consistent methodologies across studies will reduce variability and allow for more reliable comparisons of findings.

5. Conclusions

Systematic reviews and meta-analyses highlight the significant contributions of amyloid PET imaging in understanding and managing CAA. Amyloid PET reliably detects increased global and region-specific amyloid deposition in CAA patients, with a characteristic occipital-predominant pattern. However, the limitations of current imaging techniques, particularly the lack of specificity to vascular amyloids, underscore the need for continued advancements in tracer development and imaging methodologies. By addressing these challenges, amyloid PET can play an even greater role in improving the diagnosis, prognosis, and treatment of CAA.

Author Contributions: Conceptualization, M.Z. and R.P.; methodology, F.P.; formal analysis, M.Z. and R.P.; writing—original draft preparation, M.Z.; writing—review and editing, M.Z., F.P. and R.P.; supervision, R.P. All authors have read and agreed to the published version of the manuscript.

Funding: This research was funded by Ministry of University and Research (MUR), National Recovery and Resilience Plan (NRRP), project MNESYS (PE0000006)-(DN.1553 11.10.2022)M PRIMARIA Project within MNESYS framework CUP: B33C22001060002-NextGenerationEU-M4C2M; Alzheimer's Association Research Grant 23AARG-1030214, UncoveriNg Immune MechanIsms and Biomarkers of ARIA (UNIMIB-ARIA Toolkit).

Conflicts of Interest: The authors declare no conflicts of interest.

References

1. Jokinen, H.; Koikkalainen, J.; Laakso, H.M.; Melkas, S.; Nieminen, T.; Brander, A.; Korvenoja, A.; Rueckert, D.; Barkhof, F.; Scheltens, P.; et al. Global Burden of Small Vessel Disease-Related Brain Changes on MRI Predicts Cognitive and Functional Decline. *Stroke* **2020**, *51*, 170–178. [CrossRef]
2. Jansma, A.; de Bresser, J.; Schoones, J.W.; van Heemst, D.; Akintola, A.A. Sporadic cerebral small vessel disease and cognitive decline in healthy older adults: A systematic review and meta-analysis. *J. Cereb. Blood Flow Metab.* **2024**, *44*, 660–679. [CrossRef] [PubMed]
3. Wardlaw, J.M.; Smith, C.; Dichgans, M. Small vessel disease: Mechanisms and clinical implications. *Lancet Neurol.* **2019**, *18*, 684–696. [CrossRef] [PubMed]
4. Greenberg, S.M.; Bacskai, B.J.; Hernandez-Guillamon, M.; Pruzin, J.; Sperling, R.; van Veluw, S.J. Cerebral amyloid angiopathy and Alzheimer disease—One peptide, two pathways. *Nat. Rev. Neurol.* **2020**, *16*, 30–42. [CrossRef] [PubMed]
5. Charidimou, A.; Boulouis, G.; Frosch, M.P.; Baron, J.C.; Pasi, M.; Albucher, J.F.; Banerjee, G.; Barbato, C.; Bonneville, F.; Brandner, S.; et al. The Boston criteria version 2.0 for cerebral amyloid angiopathy: A multicentre, retrospective, MRI-neuropathology diagnostic accuracy study. *Lancet Neurol.* **2022**, *21*, 714–725. [CrossRef]
6. Jäkel, L.; De Kort, A.M.; Klijn, C.J.M.; Schreuder, F.H.B.M.; Verbeek, M.M. Prevalence of cerebral amyloid angiopathy: A systematic review and meta-analysis. *Alzheimers Dement.* **2022**, *18*, 10–28. [CrossRef]
7. Thal, D.R.; Attems, J.; Ewers, M. Spreading of amyloid, tau, and microvascular pathology in Alzheimer's disease: Findings from neuropathological and neuroimaging studies. *J. Alzheimers Dis.* **2014**, *42* (Suppl. S4), S421–S429. [CrossRef]
8. Jack, C.R., Jr.; Bennett, D.A.; Blennow, K.; Carrillo, M.C.; Feldman, H.H.; Frisoni, G.B.; Hampel, H.; Jagust, W.J.; Johnson, K.A.; Knopman, D.S.; et al. A/T/N: An unbiased descriptive classification scheme for Alzheimer disease biomarkers. *Neurology* **2016**, *87*, 539–547. [CrossRef]
9. Charidimou, A.; Farid, K.; Baron, J.C. Amyloid-PET in sporadic cerebral amyloid angiopathy: A diagnostic accuracy meta-analysis. *Neurology* **2017**, *89*, 1490–1498. [CrossRef]
10. Piazza, F.; Winblad, B. Amyloid-Related Imaging Abnormalities (ARIA) in Immunotherapy Trials for Alzheimer's Disease: Need for Prognostic Biomarkers? *J. Alzheimers Dis.* **2016**, *52*, 417–420. [CrossRef]
11. Loeffler, D.A. Antibody-Mediated Clearance of Brain Amyloid-β: Mechanisms of Action, Effects of Natural and Monoclonal Anti-Aβ Antibodies, and Downstream Effects. *J. Alzheimers Dis. Rep.* **2023**, *7*, 873–899. [CrossRef] [PubMed]
12. Sperling, R.A.; Jack, C.R., Jr.; Black, S.E.; Frosch, M.P.; Greenberg, S.M.; Hyman, B.T.; Scheltens, P.; Carrillo, M.C.; Thies, W.; Bednar, M.M.; et al. Amyloid-related imaging abnormalities in amyloid-modifying therapeutic trials: Recommendations from the Alzheimer's Association Research Roundtable Workgroup. *Alzheimers Dement.* **2011**, *7*, 367–385. [CrossRef] [PubMed]
13. Piazza, F.; Greenberg, S.M.; Savoiardo, M.; Gardinetti, M.; Chiapparini, L.; Raicher, I.; Nitrini, R.; Sakaguchi, H.; Brioschi, M.; Billo, G.; et al. Anti-amyloid β autoantibodies in cerebral amyloid angiopathy-related inflammation: Implications for amyloid-modifying therapies. *Ann. Neurol.* **2013**, *73*, 449–458. [CrossRef] [PubMed]
14. Zedde, M.; Pascarella, R.; Piazza, F. CAA-ri and ARIA: Two Faces of the Same Coin? *AJNR Am. J. Neuroradiol.* **2023**, *44*, E13–E14. [CrossRef]
15. Antolini, L.; Di Francesco, J.C.; Zedde, M.; Basso, G.; Arighi, A.; Shima, A.; Cagnin, A.; Caulo, M.; Carare, R.O.; Charidimou, A.; et al. Spontaneous ARIA-like Events in Cerebral Amyloid Angiopathy-Related Inflammation: A Multicenter Prospective Longitudinal Cohort Study. *Neurology* **2021**, *97*, e1809–e1822. [CrossRef]
16. Levac, D.; Colquhoun, H.; O'Brien, K.K. Scoping studies: Advancing the methodology. *Implement. Sci.* **2010**, *5*, 69. [CrossRef]
17. Tricco, A.C.; Lillie, E.; Zarin, W.; O'Brien, K.K.; Colquhoun, H.; Levac, D.; Moher, D.; Peters, M.D.J.; Horsley, T.; Weeks, L.; et al. PRISMA Extension for Scoping Reviews (PRISMA-ScR): Checklist and explanation. *Ann. Intern. Med.* **2018**, *169*, 467–473. [CrossRef]
18. Linn, J.; Halpin, A.; Demaerel, P.; Ruhland, J.; Giese, A.D.; Dichgans, M.; van Buchem, M.A.; Bruckmann, H.; Greenberg, S.M. Prevalence of superficial siderosis in patients with cerebral amyloid angiopathy. *Neurology* **2010**, *74*, 1346–1350. [CrossRef]
19. Greenberg, S.M.; Grabowski, T.; Gurol, M.E.; Skehan, M.E.; Nandigam, R.K.; Becker, J.A.; Garcia-Alloza, M.; Prada, C.; Frosch, M.P.; Rosand, J.; et al. Detection of isolated cerebrovascular beta-amyloid with Pittsburgh compound B. *Ann. Neurol.* **2008**, *64*, 587–591.

20. Clark, C.M.; Schneider, J.A.; Bedell, B.J.; Beach, T.G.; Bilker, W.B.; Mintun, M.A.; Pontecorvo, M.J.; Hefti, F.; Carpenter, A.P.; Flitter, M.L.; et al. Use of florbetapir-PET for imaging beta-amyloid pathology. *JAMA* **2011**, *305*, 275–283. [CrossRef]
21. Papanastasiou, G.; Rodrigues, M.A.; Wang, C.; Heurling, K.; Lucatelli, C.; Al-Shahi Salman, R.; Wardlaw, J.M.; van Beek, E.J.R.; Thompson, G. Pharmacokinetic modelling for the simultaneous assessment of perfusion and 18F-flutemetamol uptake in cerebral amyloid angiopathy using a reduced PET-MR acquisition time: Proof of concept. *Neuroimage* **2021**, *225*, 117482. [CrossRef] [PubMed]
22. Stroup, D.F.; Berlin, J.A.; Morton, S.C.; Olkin, I.; Williamson, G.D.; Rennie, D.; Moher, D.; Becker, B.J.; Sipe, T.A.; Thacker, S.B. Meta-analysis of observational studies in epidemiology: A proposal for reporting. *JAMA* **2000**, *283*, 2008–2012. [CrossRef] [PubMed]
23. Hozo, S.P.; Djulbegovic, B.; Hozo, I. Estimating the mean and variance from the median, range, and the size of a sample. *BMC Med. Res. Methodol.* **2005**, *5*, 13. [CrossRef]
24. Page, M.J.; McKenzie, J.E.; Bossuyt, P.M.; Boutron, I.; Hoffmann, T.C.; Mulrow, C.D.; Shamseer, L.; Tetzlaff, J.M.; Akl, E.A.; Brennan, S.E.; et al. The PRISMA 2020 statement: An updated guideline for reporting systematic reviews. *BMJ* **2021**, *372*, n71. [CrossRef]
25. Farid, K.; Charidimou, A.; Baron, J.C. Amyloid positron emission tomography in sporadic cerebral amyloid angiopathy: A systematic critical update. *Neuroimage Clin.* **2017**, *15*, 247–263. [CrossRef]
26. Charidimou, A.; Farid, K.; Tsai, H.H.; Tsai, L.K.; Yen, R.F.; Baron, J.C. Amyloid-PET burden and regional distribution in cerebral amyloid angiopathy: A systematic review and meta-analysis of biomarker performance. *J. Neurol. Neurosurg. Psychiatry* **2018**, *89*, 410–417. [CrossRef]
27. Romoli, M.; Marinoni, G.; Tagliabue, L.; Capozza, A.; Matteucci, F.; Mattone, V.; Longoni, M.; Cenni, P.; Ruggiero, M.; Rifino, N.; et al. 18FFlutemetamol-PET Aided Classification of Cerebral Amyloid Angiopathy: A Multicenter Study. *Neurology* **2024**, *103*, e209719. [CrossRef]
28. Michiels, L.; Dobbels, L.; Demeestere, J.; Demaerel, P.; Van Laere, K.; Lemmens, R. Simplified Edinburgh and modified Boston criteria in relation to amyloid PET for lobar intracerebral hemorrhage. *Neuroimage Clin.* **2022**, *35*, 103107. [CrossRef]
29. Tsai, H.H.; Pasi, M.; Tsai, L.K.; Huang, C.C.; Chen, Y.F.; Lee, B.C.; Yen, R.F.; Gurol, M.E.; Jeng, J.S. Centrum Semiovale Perivascular Space and Amyloid Deposition in Spontaneous Intracerebral Hemorrhage. *Stroke* **2021**, *52*, 2356–2362. [CrossRef]
30. Tsai, H.H.; Pasi, M.; Tsai, L.K.; Chen, Y.F.; Lee, B.C.; Tang, S.C.; Fotiadis, P.; Huang, C.Y.; Yen, R.F.; Jeng, J.S.; et al. Microangiopathy underlying mixed-location intracerebral hemorrhages/microbleeds: A PiB-PET study. *Neurology* **2019**, *92*, e774–e781. [CrossRef]
31. Yost, M.; Fiebelkorn, C.A.; Rabinstein, A.A.; Klaas, J.; Aakre, J.A.; Brown, R.D., Jr.; Mielke, M.M.; Knopman, D.S.; Lowe, V.; Petersen, R.C.; et al. Incidence of Convexal Subarachnoid Hemorrhage in the Elderly: The Mayo Clinic Study of Aging. *J. Stroke Cerebrovasc. Dis.* **2019**, *28*, 104451. [CrossRef]
32. Kim, J.; Na, H.K.; Shin, J.H.; Kim, H.J.; Seo, S.W.; Seong, J.K.; Na, D.L. Atrophy patterns in cerebral amyloid angiopathy with and without cortical superficial siderosis. *Neurology* **2018**, *90*, e1751–e1758. [CrossRef] [PubMed]
33. Baron, J.C.; Farid, K.; Dolan, E.; Turc, G.; Marrapu, S.T.; O'Brien, E.; Aigbirhio, F.I.; Fryer, T.D.; Menon, D.K.; Warburton, E.A.; et al. Diagnostic utility of amyloid PET in cerebral amyloid angiopathy-related symptomatic intracerebral hemorrhage. *J. Cereb. Blood Flow Metab.* **2014**, *34*, 753–758. [CrossRef] [PubMed]
34. Raposo, N.; Planton, M.; Payoux, P.; Péran, P.; Albucher, J.F.; Calviere, L.; Viguier, A.; Rousseau, V.; Hitzel, A.; Chollet, F.; et al. Enlarged perivascular spaces and florbetapir uptake in patients with intracerebral hemorrhage. *Eur. J. Nucl. Med. Mol. Imaging* **2019**, *46*, 2339–2347. [CrossRef] [PubMed]
35. Planton, M.; Saint-Aubert, L.; Raposo, N.; Payoux, P.; Salabert, A.S.; Albucher, J.F.; Olivot, J.M.; Péran, P.; Pariente, J. Florbetapir Regional Distribution in Cerebral Amyloid Angiopathy and Alzheimer's Disease: A PET Study. *J. Alzheimers Dis.* **2020**, *73*, 1607–1614. [CrossRef]
36. Gokcal, E.; Horn, M.J.; Becker, J.A.; Das, A.S.; Schwab, K.; Biffi, A.; Rost, N.; Rosand, J.; Viswanathan, A.; Polimeni, J.R.; et al. Effect of vascular amyloid on white matter disease is mediated by vascular dysfunction in cerebral amyloid angiopathy. *J. Cereb. Blood Flow Metab.* **2022**, *42*, 1272–1281. [CrossRef]
37. Raposo, N.; Planton, M.; Péran, P.; Payoux, P.; Bonneville, F.; Lyoubi, A.; Albucher, J.F.; Acket, B.; Salabert, A.S.; Olivot, J.M.; et al. Florbetapir imaging in cerebral amyloid angiopathy-related hemorrhages. *Neurology* **2017**, *89*, 697–704. [CrossRef]
38. Ly, J.V.; Singhal, S.; Rowe, C.C.; Kempster, P.; Bower, S.; Phan, T.G. Convexity Subarachnoid Hemorrhage with PiB Positive Pet Scans: Clinical Features and Prognosis. *J. Neuroimaging* **2015**, *25*, 420–429. [CrossRef]
39. Gurol, M.E.; Becker, J.A.; Fotiadis, P.; Riley, G.; Schwab, K.; Johnson, K.A.; Greenberg, S.M. Florbetapir-PET to diagnose cerebral amyloid angiopathy: A prospective study. *Neurology* **2016**, *87*, 2043–2049. [CrossRef]
40. Jang, H.; Jang, Y.K.; Kim, H.J.; Werring, D.J.; Lee, J.S.; Choe, Y.S.; Park, S.; Lee, J.; Kim, K.W.; Kim, Y.; et al. Clinical significance of amyloid β positivity in patients with probable cerebral amyloid angiopathy markers. *Eur. J. Nucl. Med. Mol. Imaging* **2019**, *46*, 1287–1298. [CrossRef]

41. Pyun, J.M.; Kang, M.J.; Baek, S.J.; Lee, K.; Park, Y.H.; Kim, S.Y. Magnetic Resonance Imaging-Negative Cerebral Amyloid Angiopathy: Cerebrospinal Fluid Amyloid-β42 over Amyloid Positron Emission Tomography. *J. Prev. Alzheimers Dis.* **2024**, *11*, 1041–1046. [CrossRef]
42. McCarter, S.J.; Lesnick, T.G.; Lowe, V.; Mielke, M.M.; Constantopoulos, E.; Rabinstein, A.A.; Przybelski, S.A.; Botha, H.; Jones, D.T.; Ramanan, V.K.; et al. Cerebral Amyloid Angiopathy Pathology and Its Association with Amyloid-β PET Signal. *Neurology* **2021**, *97*, e1799–e1808. [CrossRef] [PubMed]
43. Buciuc, M.; Duffy, J.R.; Machulda, M.M.; Spychalla, A.J.; Gunter, J.L.; Jack, C.R., Jr.; Giannini, C.; Raghunathan, A.; Dickson, D.W.; Josephs, K.A.; et al. Association of amyloid angiopathy with microbleeds in logopenic progressive aphasia: An imaging-pathology study. *Eur. J. Neurol.* **2021**, *28*, 670–675. [CrossRef] [PubMed]
44. Sekijima, Y.; Yazaki, M.; Oguchi, K.; Ezawa, N.; Yoshinaga, T.; Yamada, M.; Yahikozawa, H.; Watanabe, M.; Kametani, F.; Ikeda, S. Cerebral amyloid angiopathy in posttransplant patients with hereditary ATTR amyloidosis. *Neurology* **2016**, *87*, 773–781. [CrossRef] [PubMed]
45. Takahashi, Y.; Oguchi, K.; Mochizuki, Y.; Takasone, K.; Ezawa, N.; Matsushima, A.; Katoh, N.; Yazaki, M.; Sekijima, Y. Distribution and progression of cerebral amyloid angiopathy in early-onset V30M (p.V50M) hereditary ATTR amyloidosis. *Amyloid* **2023**, *30*, 109–118. [CrossRef]
46. Chatterjee, P.; Fagan, A.M.; Xiong, C.; McKay, M.; Bhatnagar, A.; Wu, Y.; Singh, A.K.; Taddei, K.; Martins, I.; Gardener, S.L.; et al. Presymptomatic Dutch-Type Hereditary Cerebral Amyloid Angiopathy-Related Blood Metabolite Alterations. *J. Alzheimers Dis.* **2021**, *79*, 895–903. [CrossRef]
47. Schultz, A.P.; Kloet, R.W.; Sohrabi, H.R.; van der Weerd, L.; van Rooden, S.; Wermer, M.J.H.; Moursel, L.G.; Yaqub, M.; van Berckel, B.N.M.; Chatterjee, P.; et al. Amyloid imaging of dutch-type hereditary cerebral amyloid angiopathy carriers. *Ann. Neurol.* **2019**, *86*, 616–625. [CrossRef]
48. Huang, C.Y.; Hsiao, I.T.; Lin, K.J.; Huang, K.L.; Fung, H.C.; Liu, C.H.; Chang, T.Y.; Weng, Y.C.; Hsu, W.C.; Yen, T.C.; et al. Amyloid PET pattern with dementia and amyloid angiopathy in Taiwan familial AD with D678H APP mutation. *J. Neurol. Sci.* **2019**, *398*, 107–116. [CrossRef]
49. Carmona-Iragui, M.; Fernández-Arcos, A.; Alcolea, D.; Piazza, F.; Morenas-Rodriguez, E.; Antón-Aguirre, S.; Sala, I.; Clarimon, J.; Dols-Icardo, O.; Camacho, V.; et al. Cerebrospinal Fluid Anti-Amyloid-β Autoantibodies and Amyloid PET in Cerebral Amyloid Angiopathy-Related Inflammation. *J. Alzheimers Dis.* **2016**, *50*, 1–7. [CrossRef]
50. Renard, D.; Collombier, L.; Demattei, C.; Wacongne, A.; Charif, M.; Ayrignac, X.; Azakri, S.; Gaillard, N.; Boudousq, V.; Lehmann, S.; et al. Cerebrospinal Fluid, MRI, and Florbetaben-PET in Cerebral Amyloid Angiopathy-Related Inflammation. *J. Alzheimers Dis.* **2018**, *61*, 1107–1117. [CrossRef]
51. Renard, D.; Tatu, L.; Collombier, L.; Wacongne, A.; Ayrignac, X.; Charif, M.; Boukriche, Y.; Chiper, L.; Fourcade, G.; Azakri, S.; et al. Cerebral Amyloid Angiopathy and Cerebral Amyloid Angiopathy-Related Inflammation: Comparison of Hemorrhagic and DWI MRI Features. *J. Alzheimers Dis.* **2018**, *64*, 1113–1121. [CrossRef] [PubMed]
52. Greenberg, S.M.; Salman, R.A.; Biessels, G.J.; van Buchem, M.; Cordonnier, C.; Lee, J.M.; Montaner, J.; Schneider, J.A.; Smith, E.E.; Vernooij, M.; et al. Outcome markers for clinical trials in cerebral amyloid angiopathy. *Lancet Neurol.* **2014**, *13*, 419–428. [CrossRef] [PubMed]
53. De Kort, A.M.; Verbeek, M.M.; Schreuder, F.H.B.M.; Klijn, C.J.M.; Jäkel, L. Prevalence of Cerebral Amyloid Angiopathy Pathology and Strictly Lobar Microbleeds in East-Asian Versus Western Populations: A Systematic Review and Meta-Analysis. *J. Stroke* **2024**, *26*, 179–189. [CrossRef] [PubMed]
54. Curtis, C.; Gamez, J.E.; Singh, U.; Sadowsky, C.H.; Villena, T.; Sabbagh, M.N.; Beach, T.G.; Duara, R.; Fleisher, A.S.; Frey, K.A.; et al. Phase 3 trial of flutemetamol labeled with radioactive fluorine 18 Imaging and neuritic plaque density. *JAMA Neurol.* **2015**, *72*, 287–294. [CrossRef]
55. Re-Read Study to Compare the Brain Uptake of [18F] Flutemetamol with Brain Neuritic Plaque Density Determined Postmortem NCT02090855. Available online: https://clinicaltrials.gov/ct2/show/NCT02090855?term=NCT02090855&rank=1 (accessed on 20 July 2014).
56. Mirra, S.S.; Heyman, A.; McKeel, D.; Sumi, S.M.; Crain, B.J.; Brownlee, L.M.; Vogel, F.S.; Hughes, J.P.; van Belle, G.; Berg, L. The Consortium to Establish a Registry for Alzheimer's Disease (CERAD). Part II. Standardization of the neuropathologic assessment of Alzheimer's disease. *Neurology* **1991**, *41*, 479–486. [CrossRef]
57. Ikonomovic, M.D.; Buckley, C.J.; Heurling, K.; Sherwin, P.; Jones, P.A.; Zanette, M.; Mathis, C.A.; Klunk, W.E.; Chakrabarty, A.; Ironside, J.; et al. Post-mortem histopathology underlying β-amyloid PET imaging following flutemetamol F 18 injection. *Acta Neuropathol. Commun.* **2016**, *4*, 130. [CrossRef]

Disclaimer/Publisher's Note: The statements, opinions and data contained in all publications are solely those of the individual author(s) and contributor(s) and not of MDPI and/or the editor(s). MDPI and/or the editor(s) disclaim responsibility for any injury to people or property resulting from any ideas, methods, instructions or products referred to in the content.